Magnetic Properties of Copper Hexadecaphthalocyanine ($F_{16}CuPc$) Thin Films and Powders

Wei Wu[1], L. A. Rochford[2], S. Felton[1], Zhenlin Wu[1], J. L. Yang[2], S. Heutz[1], G. Aeppli[3], T. S. Jones[2], N. M. Harrison[4] and A. J. Fisher[3]

Department of Materials and London Centre for Nanotechnology, Imperial College London, South Kensington Campus, London, SW7 2AZ, U.K.[1]

Department of Chemistry, University of Warwick, Coventry, CV4 7AL, U. K.[2]

UCL Department of Physics and Astronomy and London Centre for Nanotechnology, University College London, Gower Street, London WC1E 6BT, U.K.[3]

Department of Chemistry and London Centre for Nanotechnology, Imperial College London, South Kensington Campus, London, SW7 2AZ, U.K.[4]

The structural and magnetic properties of $F_{16}CuPc$ thin films and powder, including x-ray diffraction (XRD), superconducting quantum interference device (SQUID) magnetometry, and theoretical modelling of exchange interactions are reported. Analysis of XRD from films, with thickness ranging between 100 and 160 nm, deposited onto Kapton and a perylene-3,4,9,10-tetracarboxylic-3,4,9,10-dianhydride (PTCDA) interlayer shows that the stacking angle (defined in the text) of the film is independent of the thickness, but that the texture is modified by both film thickness and substrate chemistry. The SQUID measurements suggest that all samples are paramagnetic, a result that is confirmed by our theoretical modelling including density functional theory calculations of one-dimensional molecular chains and Green's function perturbation theory calculations for a molecular dimer. By investigating theoretically a range of different geometries we predict that the maximum possible exchange interaction between $F_{16}CuPc$ molecules is twice as large as that in unfluorinated copper-phthalocyanine (CuPc). This difference arises from the smaller intermolecular spacing in $F_{16}CuPc$. Our density functional theory calculation for isolated $F_{16}CuPc$ molecule also shows that the energy levels of Kohn-Sham orbitals are rigidly shifted ~1 eV lower in $F_{16}CuPc$ compared to CuPc without a significant modification of the intra-molecular spin physics, and that therefore the two molecules provide a suitable platform for independently varying magnetism and charge transport.

I. INTRODUCTION

Spintronics has attracted great interest since the discovery of giant magnetoresistance (GMR), with broad applications in information storage, magnetic sensors, biomedicine, etc.[1,2,3] Organic magnetic semiconductors, which incorporate both the charge and spin degrees of

freedom of electrons, offer a new and extremely tantalizing route towards spintronics from both the fundamental and technological points of view owing to the advantages of weak spin-orbit coupling, small hyperfine interactions and long spin-lattice relaxation time[4] as well as the prospect of easy and cheap thin-film fabrication[5]. It has recently been shown that it is possible to tune the magnetic interaction in the p-type semiconductor copper phthalocyanine (CuPc) films by controlled changes in the fabrication process [6]. The fluorinated version of CuPc, copper hexadecaphthalocyanine (F_{16}CuPc, spin-1/2) as shown in Figure 1a is an air stable n-type organic semiconductor with high charge mobility[7, 8, 9, 10, 11, 12] and is widely used in organic field-effect transistors (OFETs) and organic photovoltaics (OPVs)[13, 14, 15]. Our previous work has demonstrated thickness-dependent morphology in thermally evaporated thin films of F_{16}CuPc[16,17]. In these experiments, the crystal structure did not change as thickness increased, but morphology and texture showed a strong thickness dependence. In the thin films (thickness ~ 1 nm) the orientation of crystallites is random while thicker films (thickness ~ 80 nm) had a strong fiber crystal orientation along the (01-1) direction.

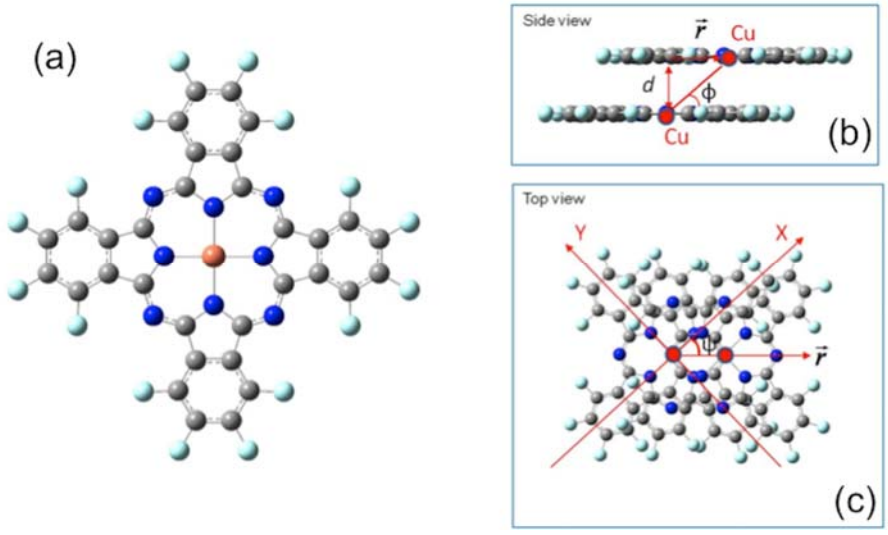


Figure 1: An isolated F_{16}CuPc molecule is shown in (a). Copper is in orange, carbon in grey, nitrogen in navy blue, and fluorine in cyan. Notice that F_{16}CuPc has a D_{4h} symmetry. A molecular dimer is shown in side view (b) and top view (c) to illustrate the important geometric parameters including the inter-plane distance d, the stacking angle φ and the sliding angle ψ. Here X = d cot(φ) cos(ψ) and Y = d cot(φ) sin(ψ).

In this paper we present a combined study of morphology, structure, and magnetic properties of F_{16}CuPc films and powder, together with density functional theory (DFT) and Green's function perturbation theory (GFPT) calculations, which have previously been shown to be in remarkably good agreement with the magnetic measurement for CuPc[18]. We find that the

F_{16}CuPc films adopt the structure recently determined in Ref.16, but that the orientation of the crystallites is affected by the thickness and the presence of an underlying layer of perylene-3,4,9,1-tetracarboxylic dianhydride (PTCDA) to produce templated films. Unlike CuPc that has a weak antiferromagnetic interaction along the chain in the thin film phase[6], F_{16}CuPc has negligible magnetic couplings in all films and powders, in agreement with our DFT results. However, a full calculation of the exchange energies as a function of intermolecular orientation suggests that F_{16}CuPc could potentially have a larger antiferromagnetic interaction than CuPc.

II. EXPERIMENTAL AND COMPUTATIONAL METHODS

A. Film growth

The F_{16}CuPc and PTCDA source materials (Sigma-Aldrich, as bought purity 80% and 97%, respectively) were purified twice by thermal gradient sublimation prior to use. The F_{16}CuPc films and PTCDA template layer were grown by high vacuum organic molecular beam deposition (OMBD) in a commercial Kurt J. Lesker SPECTROS system at a base pressure of $\sim 3\times10^{-6}$ mbar onto 25μm-thick Kapton substrates (polyimide films, 100 HN, Katco) held at ambient temperature. The thickness of F_{16}CuPc was 100 or 160 nm. To template F_{16}CuPc films, a 5 nm PTCDA layer was first deposited onto the Kapton substrate prior to growth. Thicknesses and growth rates were monitored *in situ* by calibrated quartz microbalances. Deposition rates of ~ 0.40 Å s^{-1} and ~ 0.20 Å s^{-1} were used for F_{16}CuPc and PTCDA, respectively.

B. Film morphology and structure

The morphology of the F_{16}CuPc films was characterised using field emission scanning electron microscopy (FE-SEM, Zeiss Supra 55VP). The samples were prepared for high-resolution SEM by depositing an ultrathin layer of carbon onto the sample surface to increase the conductivity of the film surface and to avoid charging. An X'Pert PRO (PANalytical) instrument with Cu K_α radiation ($\lambda \approx 1.5$ Å) operated in a θ/2θ mode was used to obtain x-ray diffraction (XRD) patterns and characterise the structure of films and powder. The scanning rate was 0.4°/min in the interval $2° \le 2\theta \le 32°$ with a step size of 0.0125°. The selected voltage and current were 45 kV and 40 mA, respectively.

C. Magnetisation measurements

The magnetic properties of F_{16}CuPc powder and films have been studied using a Quantum Design magnetic property measurement system (MPMS) superconducting quantum

interference device (SQUID) magnetometer operating in the reciprocal sample option (RSO) configuration. For the measurements on the purified powder the sample was placed in a gelatinous capsule and standard protocols were used. The techniques developed in Ref.6 were used for the measurement of thin films. The thin films were grown as narrow strips (3mm wide and 80mm long) on a flexible 25μm-thick Kapton substrate that was longer than the scanning distance of the magnetometer. The contribution from the substrate was therefore automatically compensated and subtracted from the measurement. The magnetisation of all the samples was measured both as a function of temperature and magnetic field.

D. Computational details

The molecular structure of an isolated $F_{16}CuPc$ molecule was first optimized and its electronic structure calculated using DFT implemented in the Gaussian 09 code[19] and a 6-31G basis set[20].

A one-dimensional $F_{16}CuPc$ molecular chain was modelled because the dominant electronic and magnetic interactions occur within the molecular chain[6]. The 6-31G basis set designed for use in molecular studies is inadequate to describe atomic orbitals of the copper atoms in the molecular crystal environment. To improve the description, the outer d-shell gaussian function of each copper atom in 6-31G basis set, with exponent 0.67 a_0^{-2}, was supplemented by a diffuse gaussian function with an exponent at 0.27 a_0^{-2} which is between one third and one half of the outer exponent. This successfully enhanced the basis set while avoiding pseudo-linear dependence. We used the standard 6-31G basis set for other elements in the calculations for molecular chains.

The spin-polarized DFT calculations implemented in the CRYSTAL 09 code [21] were performed to compute the exchange interaction and the electronic structure for a $F_{16}CuPc$ molecular chain. The Monkhorst-Pack sampling [22] of reciprocal space was carried out choosing a grid of shrinking factor equal to eight. The truncation of the Coulomb and exchange series in direct space was controlled by setting the Gaussian overlap tolerance criteria to 10^{-6}, 10^{-6}, 10^{-6}, 10^{-6}, and 10^{-12}.[21] The self-consistent field (SCF) procedure was converged to a tolerance of 10^{-6} atomic units (a.u.) per unit cell (p.u.c). To accelerate convergence of the SCF process, all the calculations have been performed adopting a linear mixing of Fock matrices by 30%.

Electronic exchange and correlation were approximated using the hybrid exchange-correlation functional B3LYP[23] as the inclusion of Fock-exchange partially compensates for electronic self-interaction and thus provides a reasonable description of the localization of the spin-unpaired orbitals. B3LYP has previously been shown to perform well in the calculations of exchange interactions in inorganic and organic compounds [18, 24, 25, 26, 27].

We adopted the spin Hamiltonian for a one-dimensional chain as $\hat{H} = \sum_i -2J\hat{\vec{S}}_i \cdot \hat{\vec{S}}_{i+1} + g\mu_B B\sum_i \hat{\vec{S}}_{iz}$, where J is the exchange coupling, g the Landé g-factor, μ_B the Bohr magneton, B the magnetic field, and $\hat{\vec{S}}$ the spin-1/2 operator. J was evaluated in our DFT calculations as the energy difference between the total energies of a two-molecule super-cell in which the copper spins on molecules are in the anti-ferromagnetic (AFM) and ferromagnetic (FM) configuration respectively, i.e., $J = (E_{AFM}-E_{FM})/2$. Notice that with our sign convention a negative J corresponds to an interaction favouring the AFM state (i.e., $E_{AFM}<E_{FM}$). In order to compare with DFT calculations, we adopted the formalism derived from GFPT in eq. 3 in Ref. 24 to estimate the exchange interactions qualitatively.

The intra-molecular coordinates in molecular chain were determined by the optimization of an isolated F_{16}CuPc molecule. F_{16}CuPc crystals are known to consist of parallel molecular planes along the stacking axis[16]. As shown in Figure 1b and Figure 1c, we first defined d as the inter-plane distance and $\vec{r}$ as the projection into the molecular plane of the vector joining the central copper atoms of the two molecules. Then we defined the angle between the molecular plane and the stacking axis as the stacking angle φ and the angle between $\vec{r}$ and the X axis as the sliding angle ψ. These two angles are related to the Cartesian coordinates X and Y as X=dCot(φ)Cos(ψ) and Y=dCot(φ)Sin(ψ).

It would be necessary to have a reliable description of van der Waals forces to calculate the inter-plane distance d from first principles. However, widely used exchange-correlation functionals, including B3LYP[23], do not describe van der Waals forces reliably. So in our calculations the inter-plane distance was fixed to the experimentally observed value, i.e., 3.25 Å[16] and the possible structures were generated by varying φ and ψ[24]. This value is somewhat smaller than the spacing for unfluorinated phthalocyaninces (e.g. 3.4 Å for CuPc[6]) and might be expected to result in stronger intermolecular interactions. In our calculations, the stacking angle varies from 20° to 90° and the sliding angle from 0° to 45° exploiting D_{4h} symmetry both with 5° increments.

III. RESULTS AND DISCUSSION

A. Morphology and structure

When F_{16}CuPc films were grown on Kapton substrates, a transition from spherical to high aspect ratio needle-like crystals was observed with increasing thickness. Figure 2a shows multiple crystal height profiles, suggesting a three-dimensional growth in the F_{16}CuPc 100 nm thick film. As the thickness was increased to 160 nm, similar features were observed, but their lateral size was decreased (Figure 2b). Use of a PTCDA template layer produced a film totally composed of upright needles (Figure 2c). The morphologies of films grown on Kapton were similar to those of films grown on indium tin oxide coated glass or SiO_2 substrates [16, 28].

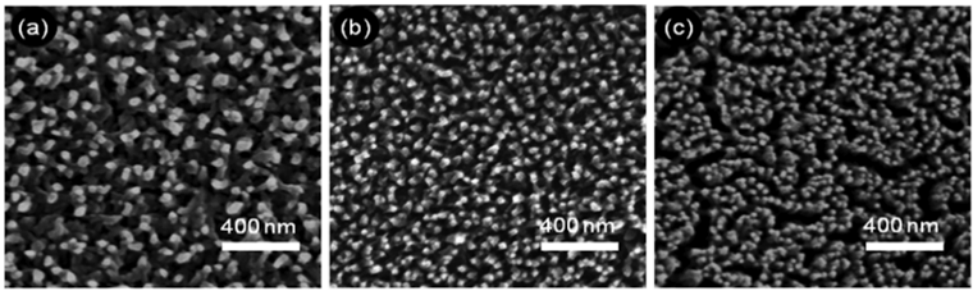


Figure 2: SEM images showing the morphology of F_{16}CuPc films grown on Kapton. (a) 100nm thick F_{16}CuPc/Kapton, (b) 160nm thick F_{16}CuPc/Kapton, (c) 160nm thick F_{16}CuPc/5 nm PTCDA/Kapton.

Figure 3 shows XRD patterns for F_{16}CuPc powder, films and a simulated pattern from single crystal diffraction data. The indexation and simulation are based on a new structure of F_{16}CuPc recently determined by our group[16]. It is similar to the one proposed by Yoon *et al.* [29], but has unit cell parameters of a = 4.89 Å, b = 10.29 Å, c = 14.91 Å, α = 74.24°, β = 87.22° and γ = 80.80° as well as an occupancy of Z = 1 implying that the arrangement of molecules in neighbouring columns does not adopt the herringbone structure. For non-templated F_{16}CuPc films, the change in film morphology with thickness was accompanied by a change in crystal texture; the 100 nm-thick F_{16}CuPc film shows a single diffraction peak at 6.2° while the 160 nm-thick films show an additional peak at 28.4°. For the templated 160 nm F_{16}CuPc film the peak at about 6.2° is not detected; instead a strong peak appears at 28.4°. This suggests purely (001) oriented crystallites in the 100nm thick non-templated film, the coexistence of (001) and (1-2-2) in the 160nm thick non-templated film, and purely (1-2-2) in the PTCDA-templated 160nm thick film. Therefore, the unit cell undergoes a 'rotation' with respect to the substrate so that the initially (001) oriented film (with stacking axis parallel to the surface) is (1-2-2) oriented after templating with the 5nm layer of PTCDA.

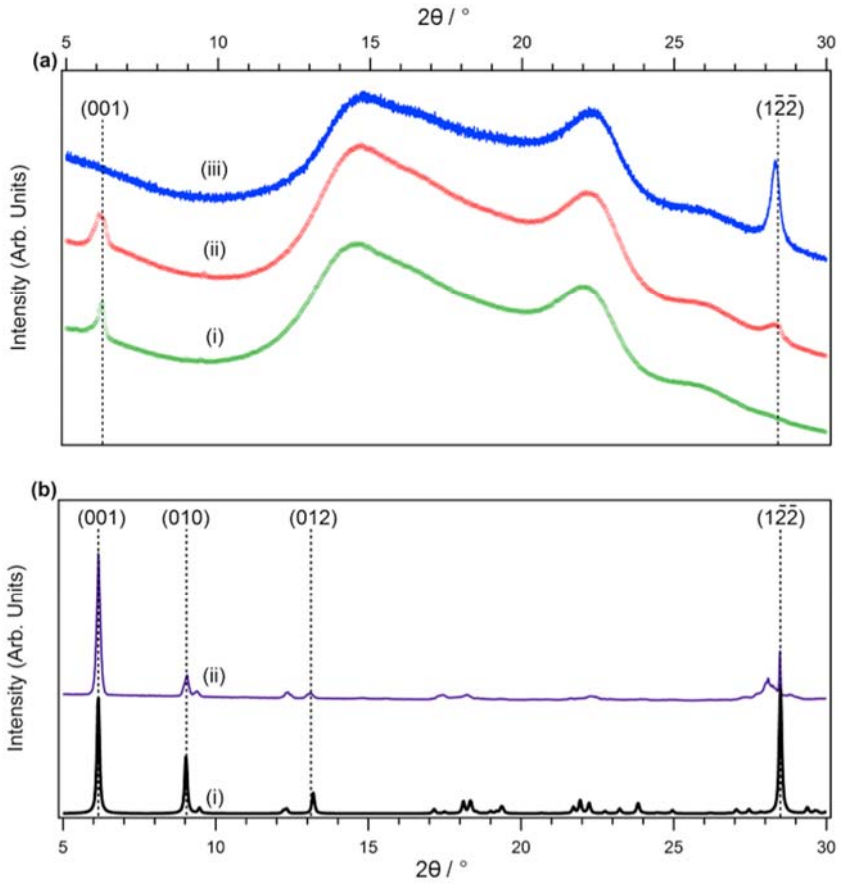


Figure 3: XRD patterns for F_{16}CuPc films grown onto Kapton (a) and for powder (b) are shown. XRD traces for F_{16}CuPc films grown onto Kapton include 100 nm thick F_{16}CuPc/Kapton in green (i), 160 nm thick F_{16}CuPc/Kapton in red (ii), and 160 nm thick F_{16}CuPc/5 nm PTCDA/Kapton in blue (iii). The broad features between 10^{o} and 27^{o} in (a) are caused by the Kapton substrate. XRD traces of F_{16}CuPc powder include a simulation in black (i) and the experimental result in purple (ii) indexed based on triclinic single crystal structure[17].

A schematic of the F_{16}CuPc molecular stacking in the two orientations adopted by the films is shown in Figure 4. The non-templated films show a strong peak corresponding to (001) orientation. This plane is therefore parallel to the substrate, and the molecules are nearly perpendicular to the substrate as shown in Figure 4a. When the F_{16}CuPc layer is grown on a 5 nm PTCDA structural template, a lack of a peak at 6.2° and the emergence of the peak at higher angle is consistent with order parallel to the (1-2-2) plane. Overall the molecular direction changes from perpendicularly oriented (Figure 4a) to close-packed along the substrate plane (Figure 4b). Based on single crystal diffraction experiments of 160nm thick film[16], each molecule is centred slightly off-axis in a triclinic cell with the π-π stacking axis along the (001) direction and molecular plane parallel to the (1-2-2) plane.

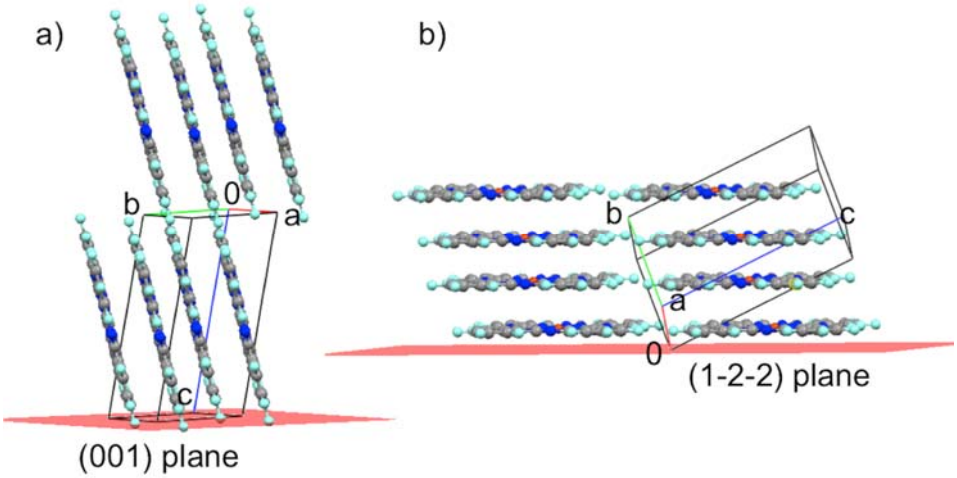


Figure 4: Schematic of the F_{16}CuPc molecules in the unit cell, showing the diffraction planes that strongly diffract in θ-2θ mode for (a) 100 nm thick films on Kapton and (b) 160 nm thick films on Kapton, and templated films on PTCDA.

B. Magnetisation measurements

In Figure 5 the magnetisation versus magnetic field (M-H) curves measured at 2 K for the different samples are shown together with the Brillouin function that simulates the behaviour of a paramagnetic material for a ½-spin with g = 2 (μ_{eff}=1.73 μ_B). The number of molecules, corresponding to the number of spin=1/2 copper centres contributing to the magnetic signal, was estimated based on the measurements of the average thickness and the knowledge of the film density. However, due to the porosity of the film (see SEM images in Figure 2), the method leads to an overestimation of the number of molecules by up to 20%. The experimental M-H curves presented in Figure 5 are therefore scaled by factors ranging between 0.95 and 0.85 so that the magnetisation at 7 T is identical in both the experimental and Brillouin curves. The small variation in the scale factor across samples prepared via different methods, which yield different orientations of the molecules in the magnetometer, is consistent with the expected isotropy of the magnetic response of the d^9 Cu^{2+} ions at the centre of the F_{16}CuPc molecules. The Brillouin function fits the experimental data very well across the whole field range showing that all the samples are paramagnetic. The experimental result is consistent with the DFT calculation which gives an interaction of J_{DFT} = -0.02 K (the theoretical result will be discussed later on), indistinguishable from zero, and therefore strongly suggests that all films adopt the same stacking angle, and that only the texture is affected by thickness and templating (Figure 4). Although we have understood the magnetic data as a whole by combining experiments with DFT calculations, our experimental data are not completely perfect. The magnetisation data for the 160 nm thick templated film revealed

a small amount of ferromagnetic contamination, which persisted to the highest measurement temperature of 150 K. The data presented here has been corrected for this contribution, by simply subtracting the experimental magnetisation data at high field and temperature for this film (3×10^{-5} emu). Since at very low fields (<0.05 Tesla) and temperature the ferromagnetic contaminant is not saturated, an artificial peak appears in the magnetisation around zero-field. However, this imperfection is only limited to very low field, which hardly affects the understanding of the whole magnetic data.

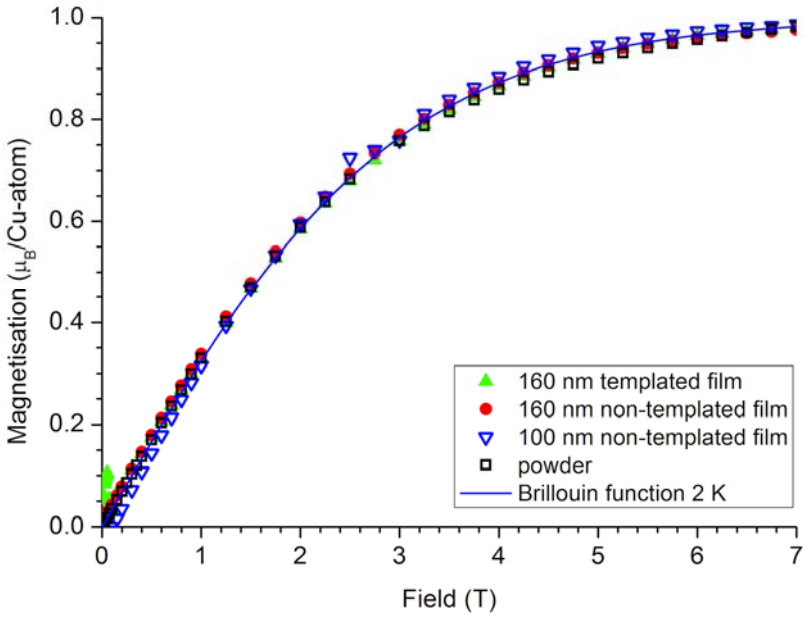


Figure 5: Magnetisation as a function of the applied magnetic field at T=2K for the three different F_{16}CuPc films and the powder. Experimental data are shown as points. The magnetization data for powder are labelled by black square, 100nm thick non-templated film by blue triangle, 160nm thick non-templated film by red solid circle, and 160nm templated film by green triangle. The solid blue curve is the Brillouin function for a ½-spin at 2 K.

C. The computed electronic structure of an isolated F_{16}CuPc molecule

The Kohn-Sham one-electron energies and orbitals of a single F_{16}CuPc molecule near the Fermi level are shown in Figure 6. The b_{1g} (an irreducible representation of D_{4h} symmetry group) state is predominantly derived from the Cu $d_{x^2-y^2}$ orbital and is singly occupied, while the doubly occupied a_{1u} state and the empty e_g states correspond respectively to the highest occupied molecular orbital (HOMO) and the lowest unoccupied molecular orbital (LUMO) in the molecular π system. The corresponding states of CuPc are readily identified; the eigenvalues in F_{16}CuPc are rigidly shifted lower by 1 eV (relative to the fixed vacuum

reference) than those of CuPc because of the much larger electronegativity of fluorine compared to hydrogen. This is consistent with previous spectroscopic studies of CuPc films with different degrees of fluorination[30]. However, the fluorine atoms hardly affect the form of the orbitals and in particular the singly occupied b_{1g} state, as they are at the outermost edge of the molecule; hence the spin polarization of the central transition metal atom is almost unchanged. This picture is consistent with the DFT calculations in Ref. 31. The mechanism for magnetic interaction between neighbouring molecules is therefore likely to be similar to that in CuPc [18], where it is dominated by indirect exchange (spin polarization of the organic ligand by the transition metal, followed by propagation of the polarization to the next molecule [18.32]).

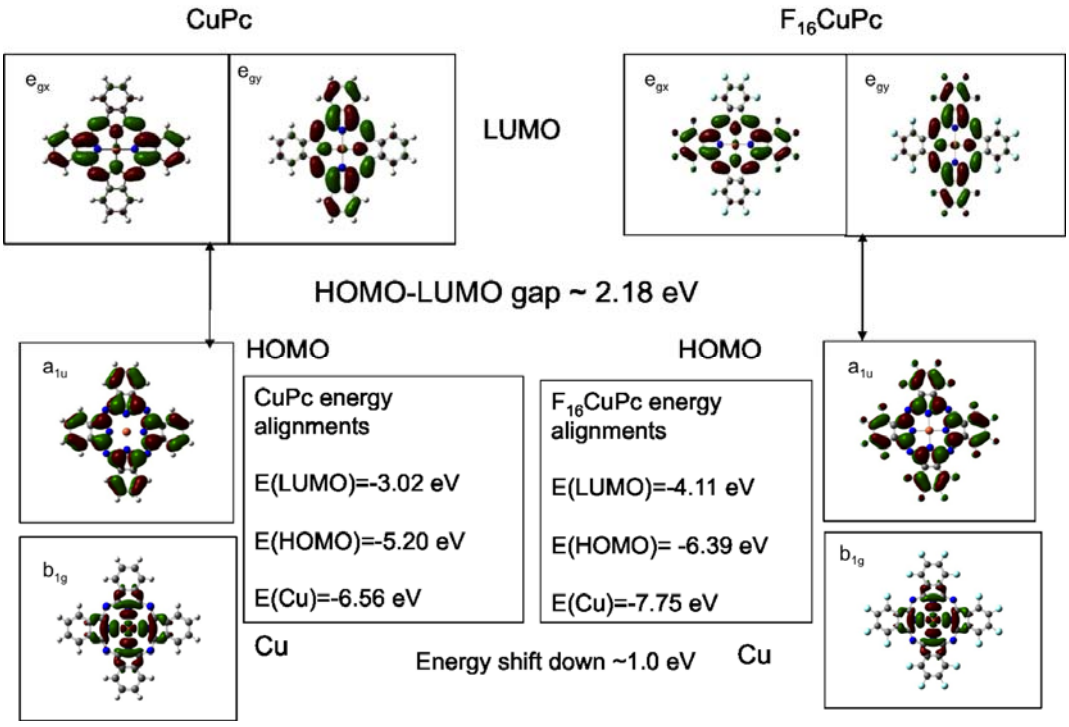


Figure 6: A comparison between the electronic structures of F_{16}CuPc (right) and CuPc (left) isolated molecules is shown. The isosurface of Kohn-Sham orbitals (positive in red and negative in green, isoval=0.001 a.u.) near the Fermi energy are plotted along with the associated irreducible representations of D_{4h} symmetry. The energy gap between HOMO and LUMO is approximately 2.18 eV. The energy level alignments of F_{16}CuPc are qualitatively the same as those of CuPc, but are rigidly shifted down by approximately 1.0 eV compared to CuPc due to the larger electronegativity of the fluorine atoms.

D. Electronic structure and exchange interactions in one-dimensional molecular chain

In Figure 7, the computed exchange interaction using DFT in a one-dimensional F_{16}CuPc chain as a function of X and Y (defined in Figure 1c) is presented. The computed exchange

interaction depends strongly on the stacking angles but weakly on the sliding angles, and increases monotonically with the stacking angles in the range of 20° to 90° with a maximum a value of ~8 K (AFM) at 90° (when the molecules are in the face-on orientation). This maximum value is almost twice as large as the maximum for CuPc[6,18,24]. We also compute the exchange interaction for the experimentally observed geometry, i.e., single crystal[16] ($\varphi \approx 42.0°$ and $\psi \approx 45°$), and find J_{DFT} = -0.02 K suggesting a paramagnetic state, in agreement with our magnetic measurements.

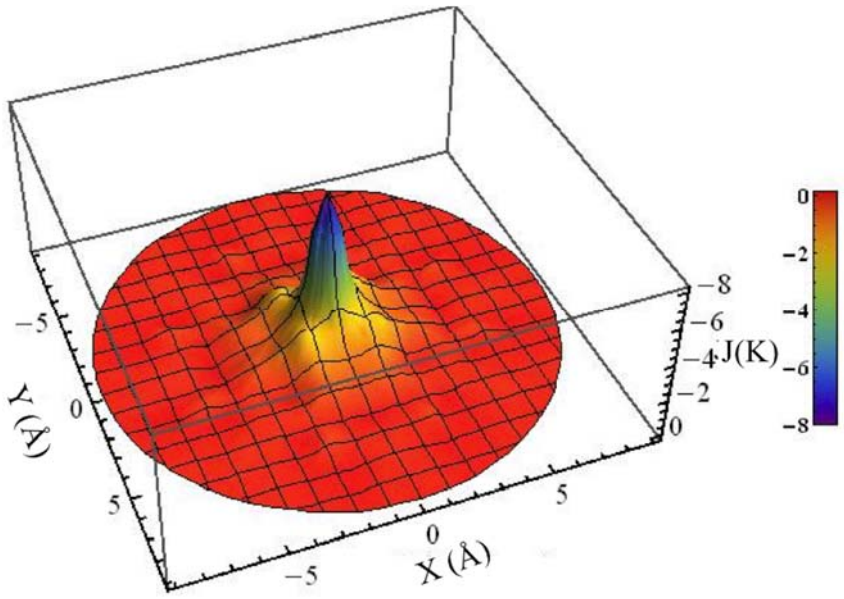


Figure 7: The exchange interaction in F_{16}CuPc calculated using DFT as a function of X and Y is shown. Notice that the computed exchange interaction depends strongly on the stacking angles, but weakly on the sliding angles. The exchange interaction peaks at a value of approximately 8.0 K (AFM).

We choose this experimental geometry as a typical example to illustrate the electronic structure of F_{16}CuPc. The band structure and density of states (DOS) of antiferromagnetic (AFM) and ferromagnetic (FM) configurations are shown in Figure 8a and Figure 8b, respectively. k_x is oriented along the stacking axis of the molecular chain and the zero of energy is chosen to be in the middle of the band gap. In DOS spin-up is displayed as positive and spin-down as negative. Eleven occupied and ten unoccupied bands of the AFM calculations are plotted from k_x=0.0 to k_x=π/a, where the lattice constant a= 9.78 Å of the magnetic super cell (double the chemical unit cell) for spin up and spin down (Figure 8a). Twelve (ten) occupied bands and nine (eleven) unoccupied bands are plotted for spin-up (spin-down) in the FM configuration (Figure 8b). The band gap is approximately 2.0 eV, which is close to the HOMO-LUMO gap in the electronic structure of the single molecule

(Figure 6); although the single-particle Kohn-Sham gap is not strictly related to an optical excitation energy, this gap is close to the Q-band optical absorption arising from the HOMO-LUMO transition in β-phase $F_{16}CuPc$[33], which has a typical wavelength of approximately 650 nm (~ 1.9 eV).

The projected density of states on the two copper atoms (PDOS) in the super-cell is plotted with spin-up in red and spin-down in blue for AFM (FM) configurations in Figure 8a (Figure 8b), and is scaled by a factor of 5 to illustrate the singly occupied orbitals. By comparing the PDOS in the AFM and FM configurations we can identify the singly occupied copper *d*-orbital from the peak positions. The singly occupied orbital derived from $d_{x^2-y^2}$ lies approximately 1.5 eV below the valence band, which is consistent with the energy alignment of the singly occupied orbital in the single-molecule electronic structure as shown in Figure 6. The Mulliken charges on the copper atoms in both the AFM and FM configurations are both approximately +0.77 |e|, and the Mulliken spin densities on the two copper atoms of the supercell in the AFM (FM) configuration are approximately 0.62 (0.62) μ_B and -0.62 (0.62) μ_B, respectively. These numbers, and the form of the band-structures themselves, are very close to the corresponding results for CuPc[24], showing once again the relatively small influence of the fluorine atoms on the spin-bearing states of the molecule. The lack of dispersion of these singly-occupied bands means the electron hopping integral between copper atoms is very small, and further indicates that it is very difficult for copper spins to interact directly through super-exchange (which would involve hopping of electrons between sites[32]). However, we can see the singly occupied band is very close to a set of ligand bands (the relatively broad bands and corresponding DOS, both shown in black) suggesting the spin polarization of the ligands due to interaction with the copper spins is facile. The gap between the singly occupied and unoccupied bands derived from the copper $d_{x^2-y^2}$ orbital provides an estimate of the on-site Coulomb interaction *U*, which is ~4 eV. This value is close to that computed in CuPc[24].

The electronic structures of the other geometries share many qualitative similarities with those in the above calculation in terms of orbital occupancy, the band gap, etc. However, their bandwidths vary significantly owing to the strong dependence of hopping integrals between the ligand π states on the geometry. These hopping integrals mediate the transfer of the spin polarization between the neighbouring molecules in the indirect exchange mechanism; hence we expect this geometry-dependent bandwidth should induce a dependence of the exchange interactions on geometry (Figure 7).

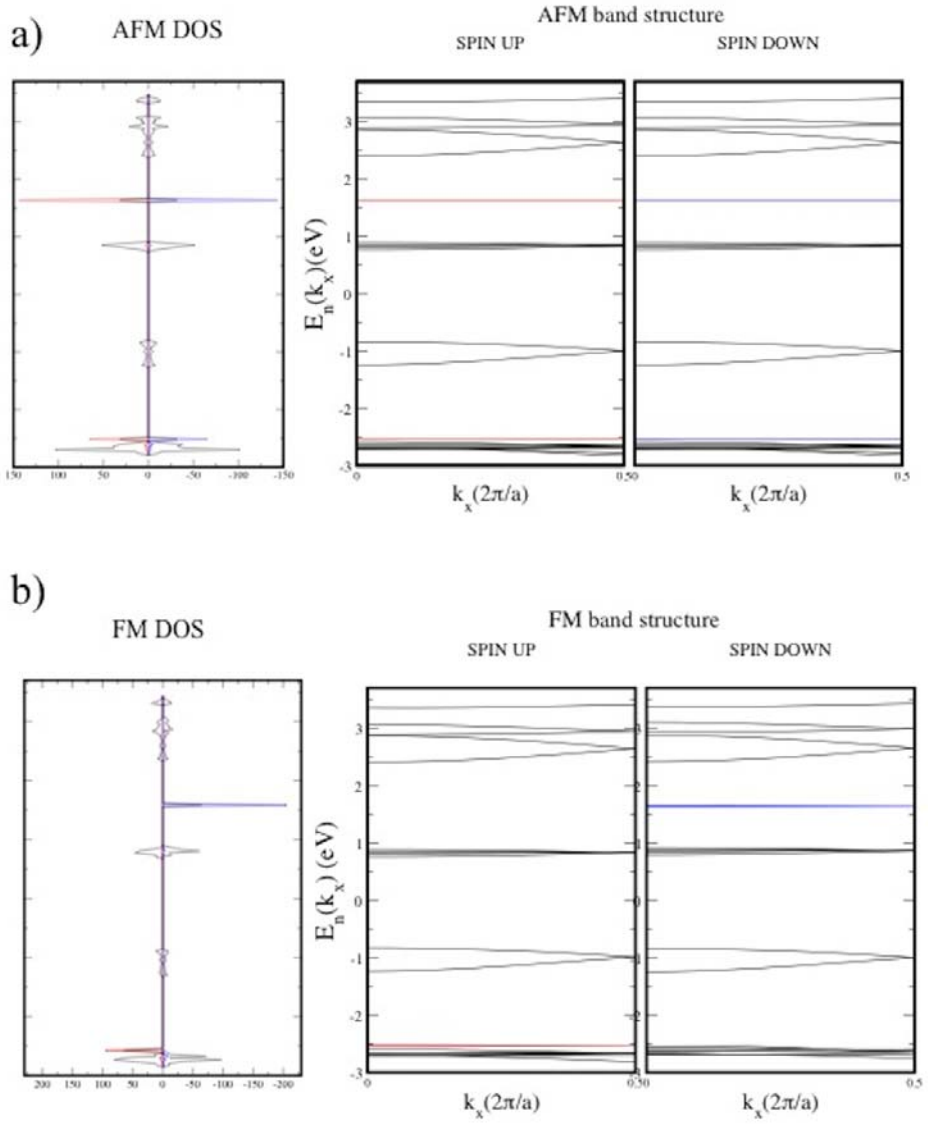


Figure 8: The band structure and density of states of a F_{16}CuPc molecular chain with the experimental geometry are shown. AFM configuration is shown in (a), and FM configuration in (b). In the band structure the bands derived from $d_{x^2-y^2}$ are highlighted in red (blue) for spin-up (spin-down). In DOS spin-up is displayed as positive and spin-down as negative. The PDOS (spin-up in red and spin-down in blue) is also shown to illustrate the singly occupied d-orbital.

We can test this correlation by using GFPT[24] to estimate the variation in exchange interactions in a dimer as a function of X and Y corresponding to the geometries used in the DFT calculations, using the hopping integrals as input. The results are once again strongly dependent on the stacking angles but weakly on the sliding angles as shown in Figure 9; the qualitative similarity to the DFT results in Figure 7 is immediately apparent. Note that only the intermolecular part of the indirect exchange is shown in Figure 9; this part will be multiplied by a prefactor arising from the intramolecular physics (polarization of the ligand

states by the copper spin), which is expected to be essentially independent of the chain geometry. Since the relevant orbitals are very similar between CuPc and F_{16}CuPc, we might also conjecture that the intramolecular terms will be similar in both systems. It is therefore interesting that the exchange interaction approximated by GFPT peaks at a stacking angle of 90° with a value of 30 arb. u. (arbitrary unit) which is twice as large as that of CuPc (Figure 6 of Ref.24 - the units, though arbitrary overall owing to the qualitative nature of GFPT formalism, are comparable between the two calculations because the local interaction between the ligand and the transition metal is similar between CuPc and F_{16}CuPc). This reflects the larger hopping integrals between ligand orbitals resulting from the smaller inter-plane spacing in F_{16}CuPc. Nevertheless the exchange for the experimental F_{16}CuPc crystal structure ($\varphi \approx 42°$ and $\psi \approx 45°$) is negligible, as in DFT. However the agreement between the two calculations is not perfect: the oscillating behaviour of exchange interactions is more prominent in perturbation theory than in DFT. This suggests that perturbation theory captures the dominant physics of the magnetic interactions between copper spins in F_{16}CuPc molecular crystals through the indirect exchange mechanism [32,34].

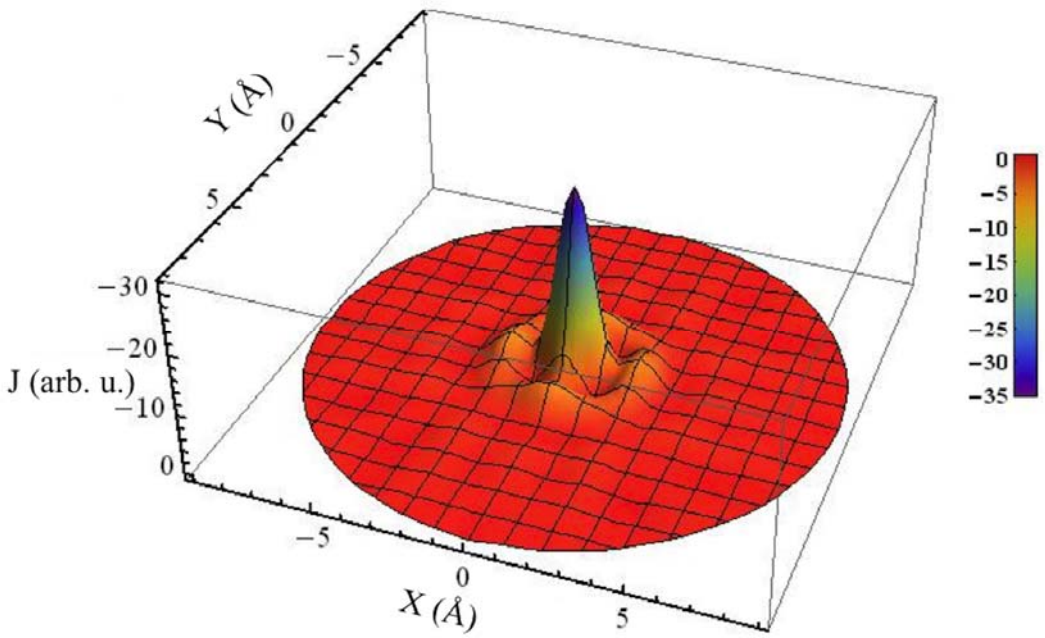


Figure 9: The exchange interaction calculated using GFPT is shown as a function of X and Y. Notice that the exchange interaction depends strongly on the stacking angle, but weakly on the sliding angle, and peaks at a value of approximately 35 arb. u..

IV. CONCLUSIONS

We report a study of F_{16}CuPc combining thin film growth, XRD analysis, SQUID magnetometry, and theoretical modelling. We show that thin films of thickness below 100 nm first adopt a (001) orientation when grown directly onto Kapton, and that for increasing thickness to 160 nm a new (1-2-2) orientation appears. The orientations correspond to the molecules lying nearly perpendicular and nearly parallel to the substrate respectively. The parallel orientation is also obtained when the films are grown onto 5 nm of PTCDA, which acts as a templating layer. Therefore, the films are shown to adopt the same stacking angle as shown in the magnetic measurement and DFT calculation, but different orientations when thickness and substrate are varied, which is in contrast to previous observations[16].

Magnetic measurements highlight that all the films and powders are paramagnetic; a single model, with uncoupled spin-1/2 moments, is consistent with the observations for all systems. The low exchange interaction is confirmed by our calculations of exchange couplings in a one-dimensional chain with experimental geometry using DFT and GFPT methods; we find J_{DFT} = -0.02 K which can be considered negligible. In comparison, the non-fluorinated CuPc films were shown to be antiferromagnetic with J ~ 2 K in the α-phase, and paramagnetic in the β-phase[6]. The stacking of the F_{16}CuPc studied here is more similar to that of β-CuPc, and therefore the low exchange constant found here is consistent with that found in the previous work on β-CuPc.

It is interesting that, despite the large difference in electronegativity between hydrogen and fluorine, the measured magnetic properties are only weakly affected by fluorination. This is readily understood from the electronic structure of the molecules: our single-molecule DFT calculation shows that the electronic structure of F_{16}CuPc is rigidly shifted 1 eV lower in energy than that of CuPc owing to the larger electronegativity of fluorine, without any significant difference in the energy gaps or the form of the orbitals.

The DFT modelling of the electronic structure of a one-dimensional F_{16}CuPc chain suggests that the spin-bearing orbital is dominantly derived from $d_{x^2-y^2}$, the band gap is approximately 2.0 eV and the on-site Coulomb interaction is approximately 4.0 eV. The calculated exchange interactions are strongly dependent on the stacking angles, but weakly on the sliding angles. These features are similar to those of CuPc as expected, but the overall scale of the exchange interactions is larger in F_{16}CuPc, with a maximum predicted value of approximately 8 K, almost doubling that in CuPc. This arises from the reduced inter-plane distance in F_{16}CuPc (approximately 0.15 Å smaller than that for CuPc). In addition, determining the inter-plane

distance at equilibrium is important for the exchange interaction. Assuming the change of the intra-molecular coordinates owing to the inter-molecular interactions can be ignored, the inter-plane distance at equilibrium could be computed by minimizing the total energy of a chain with respect to the molecular structural parameters including the inter-plane distance d, displacement r (or stacking angle φ), and sliding angle ψ in a chain. As a result, a dependence of the equilibrium inter-plane distance on the displacement (or the stacking angle) and the sliding angle can be established.

It is noteworthy that DFT and GFPT exchange calculations agree qualitatively with one another, both for the structural trends of each material and for the differences between the two molecules. Without such agreement the total energy differences computed within DFT could be considered negligibly small, since they rely heavily on cancellation of much larger errors; the agreement with GFPT shows that essentially the same results arise from a method which focuses directly on the small energy differences, and also confirms that the physical origin of the magnetic interaction is indirect exchange, as in CuPc.

Our combined study implies that although it is paramagnetic in the current structure, F_{16}CuPc could potentially have exchange couplings that surpass those in CuPc. The distinct electronic properties compared to CuPc, in particular the shift in the one-electron spectrum, would also allow charge transport and spin coupling to be tuned independently in CuPc/F_{16}CuPc structures.

V. ACKNOWLEDGEMENT

We thank the Research Council UK and the Engineering and Physical Sciences Research Council (EPSRC) for financial support through the Basic Technology grant "Molecular Spintronics" (EP/F04139X/1; EP/041160/1; EP/F041349/1). ZW and SH thank the EPSRC for a First Grant (EP/F039948/1). We thank Chris Kay, Michele Serri, James Stott, and Marc Warner for helpful discussions.

VI. REFERENCES

[1] G. A. Prinz, Phys. Today **48**(4), 58 (1995).

[2] G. A. Prinz, Science **282**, 1660 (1996).

[3] S. A. Wolf, D. D. Awschalom, R. A. Buhrman, J. M. Daughton, S. S. von Molnar, M. L. Rouke, A. Y. Chtchelkanova and D. M. Treger, Science **294** ,1488 (2001).

[4] S. Pramanik, C.-G. Stefanita, S. Patibandla, S. Bandyopadhyay, K. Garre, N. Harth and M. Cahay, Nat. Nano. **2** 216 (2007).

[5] Editorial, Nat. Mat. **8**, 691 (2009).

[6] S. Heutz, C. Mitra, Wei Wu, A. J. Fisher, A. Kerridge, A. M. Stoneham, A. H. Harker, J. Gardener, H.-H. Tseng, T. S. Jones, C. Renner, and G. Aeppli, Adv. Mater. (Weinheim, Ger.) **19**, 3618–3622 (2007).

[7] Z. Bao, A. J. Lovinger, and J. Brown, J. Am. Chem. Soc. **120**, 207 (1998).

[8] H. B. Wang, F. Zhu, J. L. Yang, Y. H. Geng, and D. H. Yan, Adv. Mater. **19**, 2168 (2007).

[9] Q. Tang, H. Li, Y. Liu, and W. Hu, J. Am. Chem. Soc. **128**, 14634 (2006).

[10] J. Wang, H. Wang, X. Yan, H. Huang, and D. Yan Appl. Phys. Lett. **87**, 093507 (2005).

[11] J. Wang, H. Wang, X. Yan, H. Huang, D. Jin, J. Shi, Y. Tang, and D. Yan, Adv. Funct. Mater. **16**, 824 (2006).

[12] X. Jiang, J. Dai, H. Wang, and Y. Geng, D. Yan, Chem. Phys. Lett. **446**, 329 (2007).

[13] B. Crone, A. Dodabalapur, Y. Y. Lin, R. W. Filas, Z. Bao, A. Laduca, R. Sarpeshkar, H. E. Katz, and W. Li, Nature (London) **403**, 521 (2000).

[14] H. Edzer, A. Huitema, G. H. Gelinck, J. Bas, P. H. Van Der Putten, K. E. Kuijk, K. M. Hart, E. Cantatore, and D. M. De Leeuw, Adv. Mater. (Weinheim, Ger.) **14**, 1201 (2002).

[15] J. L. Yang, S. Schumann, R.A. Hatton, and T. S. Jones, Org. Electron. **11**, 1399 (2010).

[16] P. A. Pandey, L. A. Rochford, D.S. Keeble, J. P. Rourke, T. S. Jones, R. Beanland and N. R. Wilson, Chem. Mater. **24**, 1365 (2012).

[17] J. L. Yang, S. Schumann, and T. S. Jones, J. Phys. Chem. C. **114**, 1057 (2010).

[18] Wei Wu, A. Kerridge, A. H. Harker, and A. J. Fisher, Phys. Rev. B **77** 184403 (2008).

[19] M. J. Frisch, et. al., Gaussian 09 (Gaussian, Inc., Pittsburgh, PA, 1998).

[20] R. Ditchfield, W. J. Hehre, and J. A. Pople, J. Chem. Phys.**54**, 724 (1971).

[21] R. Dovesi, V. R. Saunders, C. Roetti, R. Orlando, C. M. Zicovich-Wilson, F. Pascale, B. Civalleri, K. Doll, N. M. Harrison, I. J. Bush, P. D'Arco, and M. Llunell, CRYSTAL09 User's Manual (University of Torino, Torino, 2009).

[22] H. J. Monkhorst and J. D. Pack, Phys. Rev. B **13**, 5188 (1976).

[23] A. D. Becke, J. Chem. Phys. **98**, 5648 (1993).

[24] Wei Wu, A. J. Fisher, and N. M. Harrison, Phys. Rev. B **84** 024427 (2011).

[25] F. Illas, I de P.R. Moreira, C. de Graaf and V. Barone, Theo. Chem. Acc. **104**, 265 (2000).

[26] G. C. De Fusco, L. Pisani, B. Montanari, and N. M. Harrison, Phys. Rev. B **79**, 085201 (2009).

[27] G. C. De Fusco, B. Montanari, and N. M. Harrison, Phys. Rev. B **82**, 220404(R) (2010).

[28] J. L. Yang, S. Schumann, and T.S. Jones, J. Mater. Chem. 21, 5812 (2011)..

[29] S. M. Yoon, H. H. Song, I. C. Hwang, K. S. Kim, and H. C. Choi, Chem. Commun. 2010, **46**, 231-233.

[30] H. Peisert, M. Knupfer, T. Schwieger, G. G. Fuentes, D. Olligs, J. Fink and Th. Schmidt, J. Appl. Phys. **93**, 9683 (2003).

[31] D. G. de Oteyza, A. El-Sayed, J. M. Garcia-Lastra, E. Goiri, T. N. Krauss, A. Turak, E. Barrena, H. Dosch, J. Zegenhagen, A. Rubio, Y. Wakayama, and J. E. Ortega, J. Chem. Phys. **133**, 214703 (2010).

[32] P. W. Anderson, Phys. Rev. **115**, 2 (1959).

[33] M. I. Alonso, M. Garriga, J. O. Ossó, F. Schreiber, E. Barrena, and H. Dosch, J. Chem. Phys. **119**, 6335 (2003).

[34] M. A. Ruderman and C. Kittel, Phys. Rev. **96**, 99 (1954).